

# **DOE-FIU SCIENCE & TECHNOLOGY WORKFORCE DEVELOPMENT PROGRAM**

## **STUDENT SUMMER INTERNSHIP TECHNICAL REPORT- SUMMER 2009**

June 1, 2009 to August 7, 2009

### **Verification and Validation of the AMROC Fluid Solver Framework Coupling with DYNA3D within the Virtual Test Facility Fluid Structure Interaction Suite**

#### **Principal Investigators :**

Stephen Wood (DOE Fellow Student)  
Florida International University

Dr. Ralf Deiterding, Mentor  
Oak Ridge National Laboratory

#### **Acknowledgements:**

Dr. Ralf Deiterding

#### **Florida International University Collaborator:**

Leonel Lagos Ph.D., PMP®

#### **Prepared for:**

U.S. Department of Energy  
Office of Environmental Management  
Under Grant No. DE-FG01-05EW07033

### **DISCLAIMER**

This report was prepared as an account of work sponsored by an agency of the United States government. Neither the United States government nor any agency thereof, nor any of their employees, nor any of its contractors, subcontractors, nor their employees makes any warranty, express or implied, or assumes any legal liability or responsibility for the accuracy, completeness, or usefulness of any information, apparatus, product, or process disclosed, or represents that its use would not infringe upon privately owned rights. Reference herein to any specific commercial product, process, or service by trade name, trademark, manufacturer, or otherwise does not necessarily constitute or imply its endorsement, recommendation, or favoring by the United States government or any other agency thereof. The views and opinions of authors expressed herein do not necessarily state or reflect those of the United States government or any agency thereof.

## ABSTRACT

---

The simulation of shock-loaded thin walled structures requires numerical methods that can cope with large deformations as well as local topology changes. A software suite capable of simulating shock loaded structures can be utilized to examine pipeline unplugging phenomena. We present a comparison of solid mechanics simulations and fluid-structure interaction (FSI) simulations of exemplary test cases as part of a verification and validation procedure to extend the functionality of the Virtual Test Facility (VTF) by incorporating DYNA3D. The VTF developed by Deiterding et al. is a generic software framework for shock-driven FSI simulation that imposes embedded moving wall boundary conditions on a Cartesian fluid solver with a ghost fluid approach. DYNA3D is a nonlinear, explicit finite element code for analyzing the transient dynamic response of three-dimensional solids and structures. The fluid solver, AMROC (Adaptive Mesh Refinement in Object Oriented C++), and the solid solver, DYNA3D, exchange data only at the interface between disjointed computational domains after consecutive time steps. The first test case selected is the verification configuration of a thin-walled steel panel impacted by a planar shockwave in air. This test case can be modeled as a one-dimensional elastic beam immersed in a two-dimensional fluid domain where the Euler-Bernoulli beam equation can be used to calculate the deflection of the beam middle axis with updated hydrodynamic loading after every AMROC time step. Results from the coupled AMROC-DYNA solver agree well with analytic results. The validation test cases involve viscoplastic deformation and fracture of thin circular isotropic metal plates subjected to shock loadings from or similar to underwater explosions. Independent DYNA3D simulations with approximate pressure loads exhibit comparable amplitudes of plastic deformation with over-predicted rates of deformation. AMROC-DYNA results, however, reveal a significant reduction in loading caused by cavitation following the impact of the pressure wave on the plate. Further, following cavitation, the coupled simulations exhibit a region of increasing pressure at the plate. These computations also agree much better with experimental results than independent solid solver simulations that do not consider the alteration of the pressure boundary conditions due to FSI. DYNA3D's successful integration into the VTF by the addition of pre- and post-processing routines and by the verification and validation tests has produced a robust software suite for investigating shock-driven FSI phenomena. Continued development extending AMROC-DYNA to thick walled and arbitrary structures matched with experiments to correlate plug material parameters will produce a robust tool for investigating pipe unplugging phenomena.

## TABLE OF CONTENTS

---

LIST OF FIGURES .....	v
LIST OF TABLES .....	v
1. INTRODUCTION .....	1
2. EXECUTIVE SUMMARY .....	6
3. RESEARCH DESCRIPTIONS .....	9
4. RESULTS AND ANALYSIS .....	20
5. CONCLUSION .....	29
6. REFERENCES .....	30

## LIST OF FIGURES

---

Figure 1. Example test-bed configuration.....	2
Figure 2. K-Mag plug. ....	2
Figure 3. Hydraulic extrusion test.....	3
Figure 4. Torsion shear vane test. ....	3
Figure 5. Example performance evaluation results.....	3
Figure 6. AMROC grid refinement hierarchy.....	10
Figure 7. AMROC regridding strategy. ....	10
Figure 8. Uni-axial stress-strain relationship. ....	12
Figure 9. AMROC-DYNA data flow.....	13
Figure 10. Coupling surface.....	14
Figure 11. Generation of a cohesive element.....	16
Figure 12. Node selection sets. ....	16
Figure 13. Generated cohesive elements. ....	17
Figure 14. Verification Test Case computational domain. ....	18
Figure 15. AMROC-DYNA validation experimental setup. ....	19
Figure 16. Comparison of the traveling wave approximation (dotted) with computed pressure traces (solid) at $x_1 = 1.1$ m (left) and $x_1 = 0.2$ m (right). ....	19
Figure 17. DYNA3D verification. ....	20
Figure 18. AMROC-DYNA panel displacement.....	21
Figure 19. AMROC-DYNA verification. ....	22
Figure 20. AMROC-DYNA verification panel motion coupled field results.....	23
Figure 21. Pressure traces along centerline.....	24
Figure 22. Plate centerline x-displacement. ....	24
Figure 23. Fluid pressure distribution revealing cavitation and stressXX distribution within the copper plate at $t = 0.15$ ms. ....	25
Figure 24. Comparison of AMROC-DYNA results with experiment results.....	26
Figure 25. Comparison of AMROC-DYNA fracture demonstration with experimental results. ....	26
Figure 26. Fluid density and plate von Mises stress. ....	27
Figure 27. Fluid pressure and plate von Mises stress from behind the plate in left column and from in front of the plate in the right column. ....	28

## LIST OF TABLES

---

Table 1. Simulant Plug Materials.....	2
---------------------------------------	---

# 1. INTRODUCTION

---

## 1.1 Un-Plugging Background

The Department of Energy (DOE) Hanford Site in Richland, Washington, is adjacent to the only portion of the Columbia River which is still free-flowing. The surrounding area of the Mid-Columbia Valley is one of the few without modern agricultural development and is revered by local American Indian tribes for its spiritual and cultural importance. The United States Government acquired land for the Hanford Site in 1943 to build large industrial facilities to produce plutonium, which played a major role in the nation's defense and in bringing about the end of World War II. The legacy high level waste from the initial production activities during WW II and the expanded operations at the site during the Cold War have been stored in 149 single-shell tanks, many of which date back to the 1940's.

“Removing the waste from the single-shell tanks and upgrading the aging infrastructure in the tank farms is a top priority for the Department of Energy, a necessary step to protect the Columbia River, and key to providing tank waste feed to the Hanford vitrification plant in 2019,” said Office of River Protection Manager Shirley J. Olinger. (Office of River Protection). Twenty-eight (28) double-shell tanks have been constructed at the site as part of the infrastructure improvements. The waste is an amalgam of liquids and solids which have settled and stratified inside the tanks. Technologies are employed and under development to re-suspend the particulates in solution to facilitate pumping and transfer to double-shell tanks. However, the transfer lines at times become plugged by the solids which adhere to the pipeline walls.

## 1.2 FIU-ARC Full Scale Testing

Since the Fall 2008 semester, the DOE Fellow, Stephen Wood, has assisted with the testing of industry pipeline unplugging technologies through the DOE/FIU Science & Technology Workforce Initiative program at FIU's Applied Research Center. The objectives of the full scale testing endeavor are to:

1. Assist DOE with pipeline unplugging technology evaluation and qualification
2. Provide an understanding of the underlying physics of each technology
  - a. Propagation of pressure pulses
  - b. Effects of pipeline configurations
    - i. Bends
    - ii. Expansion loops
    - iii. Valves and other fixtures
3. Determine whether the technology can unplug a pipeline blocked 19,000 ft from the inlet where the technology attaches to the pipeline

An example of the pipeline configuration utilized in full scale testing is shown in Figure 1. The test-bed shown was utilized to evaluate NuVision's unplugging technology.

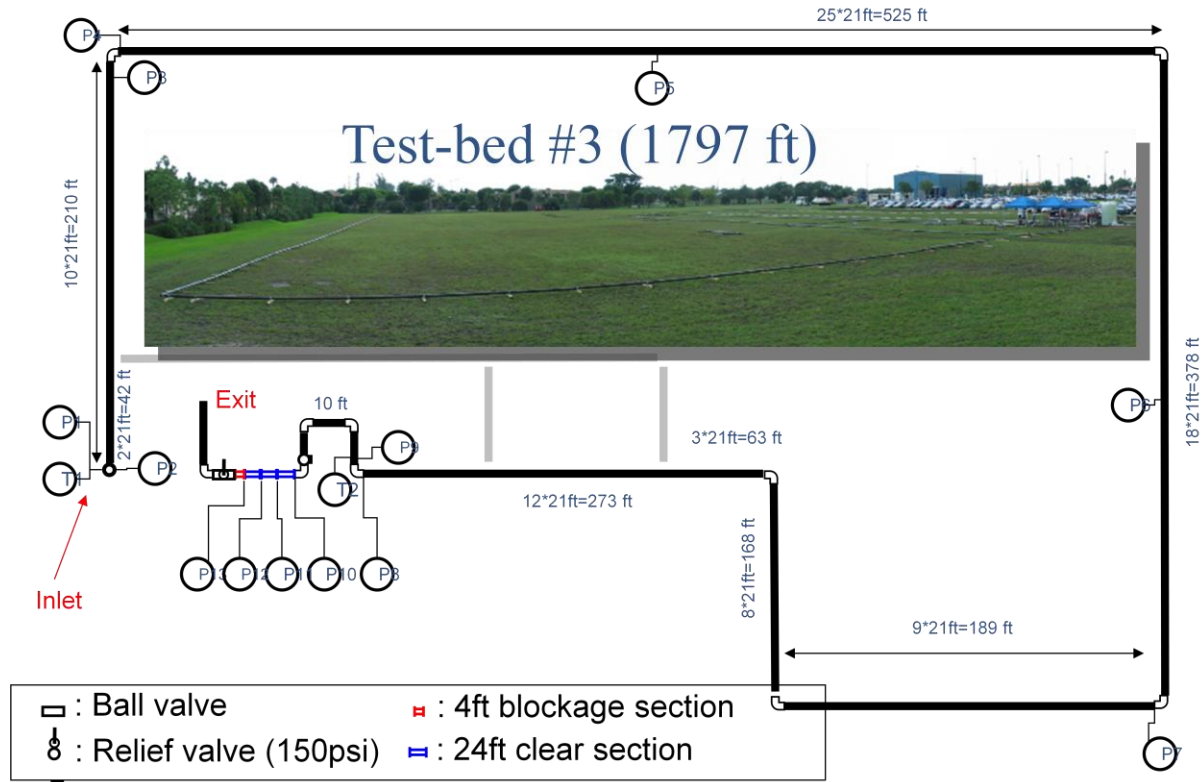


**Figure 1. Example test-bed configuration.**

The waste materials which have been observed conglomerating in single-shell tanks and the associated pipelines have been represented by simulant plugs for the tests administered at FIU-ARC. The simulant materials exhibit mechanical properties which exemplify the mechanical responses in unplugging events in the field while providing a radiation and chemical hazard-free test environment. Table 1 lists the materials used in simulant plugs for two companies, NuVision and AIMMS.

**Table 1. Simulant Plug Materials**

NuVision	AIMMS
Kaolin	Bentonite
Aluminum Gel	NaAlSi
Phosphate Gel	K-Mag



**Figure 2. K-Mag plug.**

To ensure the accuracy and consistency of the tests performed, each batch of simulant plugs is subjected to quality control and quality assurance testing, including hydraulic extrusion, torsion shear vane, and penetrator testing. Figure 3 and Figure 4 show the hydraulic extrusion test and the torsion shear vane test, respectively.

Testing an unplugging technology consists of performance evaluation and parameter variation to obtain data for qualification and analysis. Figure 5 shows a selection of data gathered from one of the performance evaluation tests on the AIMMS' technology.



**Figure 3. Hydraulic extrusion test.**



**Figure 4. Torsion shear vane test.**

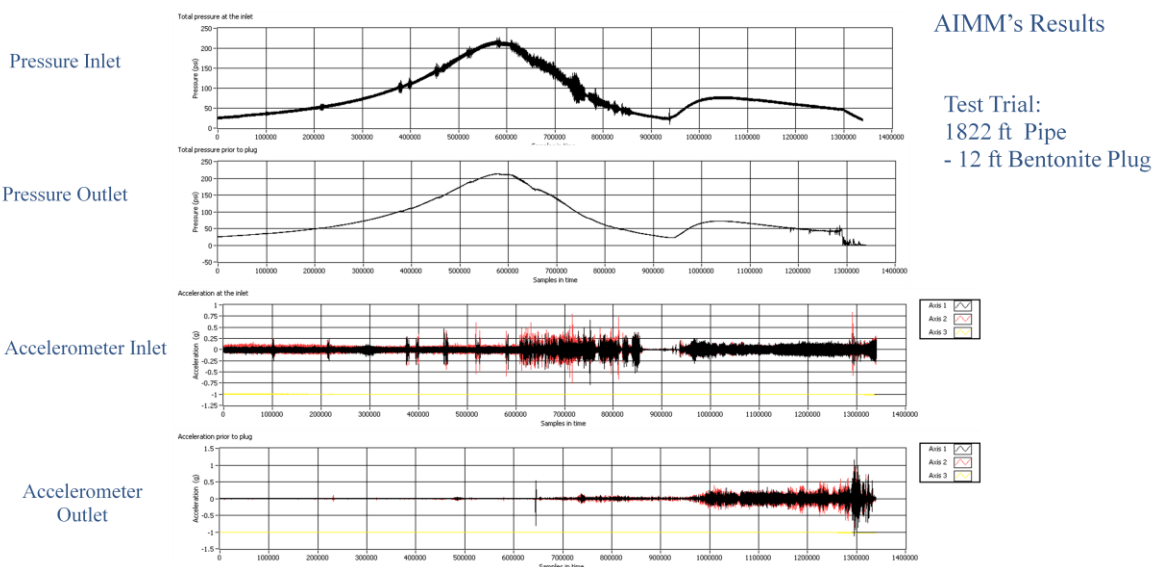


**Figure 5. Example performance evaluation results.**

### 1.3 Fluid Structure Interaction

Analysis of the pressure transducer and accelerometer data gathered from performance and parameter variation tests provided limited insight into the fluid structure interaction phenomenon which were able to unplug simulant plugs. The extrusion of some simulant plugs and the erosion of others did not directly correlate with the varied technology parameters. While the data and analysis was sufficient to qualify the tested technologies, it gave rise to questions regarding the interaction and effectiveness of the waves, pressure pulses, and air injections with the simulant plugs and the pipeline.

Fluid structure interaction (FSI) is the study of deformable structures with surrounding and/or internal fluid flows. This field of FSI has traditionally been applied to such engineering applications as the stability and response of aircraft wings, the flow of blood through arteries, the response of bridges and tall buildings to winds, the vibration of turbine and compressor blades, and the oscillation of heat exchangers. In all of these applications, the structure deformations are small (purely plastic) and, in most, the goal is to develop systems which minimize the deformations and provide stable performance. These criteria and goals have tailored the software tools which have been developed to be very efficient for such situations and unsuitable for applications involving large structure deformations (visco-plastic elastic) where fracture may occur.

### 1.4 Summer Internship Objectives

This summer, the DOE Fellow participated in an internship at the Oak Ridge National Laboratory (ORNL) through the DOE-FIU Science & Technology Workforce Development Initiative. Thanks to guidance from Dr. Lagos of FIU's Applied Research Center (ARC) and Prof. Dulikravich, and the work of the ORISE staff, in particular Ms. Vicki Heidle, the DOE Fellow was able to work with Dr. Ralf Dieterding at ORNL. While there, the DOE Fellow extended the capabilities of and performed verification and validation on a fluid-structure interaction software suite, the Virtual Test Facility.

The Virtual Test Facility (VTF) is a source code collection of compressible computational fluid dynamics (CFD) and computational solid dynamics (CSD) solvers. The CFD solvers facilitate the computation of flows with strong shocks as well as fluid mixing. The CSD solvers provide capabilities for simulation of dynamic response in solids such as large plastic deformations, fracture and fragmentation. In addition, the VTF can be used to simulate highly coupled fluid-structure interaction problems, such as the high rate deformation experienced by a metallic solid target forced by the loading originating from the detonation of energetic materials, or the rupture and fragmentation of brittle materials under shock wave impact. At present, all VTF solvers use time-explicit numerical methods that track the various wave phenomena responsible for mediating the dynamic response through the application of suitable numerical methods. AMROC (Adaptive Mesh Refinement in Object-oriented C++), developed by Dr. Ralf Dieterding, is the fluid solver framework within the VTF software suite.

Recently, the work to add a new CSD, DYNA3D, to the VTF suite was begun. DYNA3D is an explicit finite element program for structural/continuum mechanics problems developed by Lawrence Livermore National Laboratory. DYNA3D's material library includes isotropic elastic, orthotropic elastic, elastic-plastic, orthotropic elastic-plastic, rate-dependent elastic-plastic, temperature-dependent elastic-plastic, concrete, and rubber-like materials. Its element library includes solid, shell, beam, bar, cohesive, and damper elements. DYNA3D also has various contact surface options for interaction effects between two bodies (Lawrence Livermore National Laboratory, 2009).

In May 2009, the coupling of DYNA3D to AMROC had been completed but not verified or validated. An efficient procedure for generating the input files for DYNA3D still needed to be developed and implemented along with a method for post processing the coupled results of AMROC and DYNA3D.

The objectives of the DOE Fellow's internship with Dr. Deiterding were to:

1. Select, run, and document test cases that they are analytically accessible for verification
2. Select, run, and document test cases from published experimental results for validation
3. Explore capabilities of DYNA3D
  - a. Element types
  - b. Material types
  - c. Solver parameters
4. Explore capabilities of coupled AMROC-DYNA FSI Solver
  - a. Element types
  - b. Material types
  - c. Solver parameters
    - i. Level Set Generation
    - ii. DYNA3D sub iterations
5. Develop and implement a geometry pre-processor routine
6. Develop and implement a DYNA3D post-processor routine

## 2. EXECUTIVE SUMMARY

---

### 2.1 Summer Internship Objectives

This summer, the DOE Fellow, Stephen Wood, participated in an internship at the Oak Ridge National Laboratory (ORNL) through the DOE-FIU Science & Technology Workforce Development Initiative. Thanks to guidance from Dr. Lagos of FIU's Applied Research Center (ARC) and Prof. Dulikravich, and the work of the ORISE staff, in particular Ms. Vicki Heidle, the DOE Fellow was able to work with Dr. Ralf Dieterding at ORNL. While there, the DOE Fellow extended the capabilities of and performed verification and validation on a fluid-structure interaction software suite, the Virtual Test Facility.

### 2.2 Methodology

A literature search of FSI software validation and FSI experimental publications was undertaken in parallel with an examination of the DYNA3D manuals, examples, and publications cited by the developers. Test cases were selected from the literature surveyed which had detailed material data and results for the plastic and elastic response of a structure subjected to a strong shock in water or air.

A geometry pre-processor routine was developed and implemented which reads the Abaqus format CUBIT export file containing the nodes, elements, and node selection sets. The routine identifies the element types present, then applies nodal boundary conditions (B.C.) from the B.C. node selection sets, and then searches for element faces to form the coupling surface with AMROC from the pressure load node selection sets.

For the initial verification of the implementation of DYNA3D, low to moderate loading was applied to the steel panel structure to yield purely elastic responses. Accordingly, elastic materials were applied within the simulation. For higher loadings, viscoplastic/elastic and failure material types were evaluated for their accuracy and computational cost.

As the interaction of stronger shock with structures were examined and experimental results indicated fracture was likely, DYNA3D's cohesive elements were tested and implemented within the pre-processor through a cohesive node selection set. To produce stable solutions for these simulations of higher deformation rates, several DYNA3D solver parameters had to be examined and fine tuned. Most prominent of these being the set of hour-glass stabilization parameters, the time-step scale factor, the slide surface coefficients, and the cohesive element properties.

For cases where the fluid structure interaction caused the structure to fracture, the capabilities of the level-set generation algorithm with AMROC were explored.

In order to visualize the coupled results of the fluid and structure interaction, an output format which would allow superimposed data sets had to be found. The Visualization Toolkit (VTK) format based on open source C++ libraries developed by the VTK project (Visualization Tool Kit, 2009) was selected for its wide portability. VisIt, a free interactive parallel visualization and graphical analysis tool developed by the DOE Advanced Simulation and Computing Initiative (ACSI) (Lawrence Livermore National Laboratory, 2009), was selected to view the coupled data. A routine to retrieve and translate the displacements, velocities, and stresses from the DYNA3D data structures into VTK format was developed and implemented.

## 2.3 Results

The brick element type was found to be the most accurate solid element type for the high deformation and strain rates present in both test cases. The release of DYNA3D utilized also supports five quadrilateral 4-node shell elements which can be degenerated to a triangular three-node element, but at the expense of accuracy. The triangular elements formed from collapsed quadrilaterals were found to lock due to excessive transverse shear, yielding non-physical results. The quadrilateral four-node shell and eight-node “brick” elements produced results which are in good agreement with the Euler-Bernoulli beam equation and each other. The same element types produced results in good agreement with the experimental results from the plate deformation from water hammer experiments.

Cases where the fluid structure interaction caused high rates of deformation in thin structures and ultimately fracture were simulated successfully for thin structures modeled with solid hexagonal elements, cohesive elements, and slide surfaces. The restriction to thin structures, that is those structures which can be represented in the fluid domain by unsigned distance functions, is enforced because at present the algorithm implemented to generate the level sets from the solid surface does not capture new surfaces along crack faces. The results obtained are in agreement with the observed experimental results.

The geometry pre-processor routine functions robustly for multiple bodies and element types. The test cases employed for verification and validation were of single body, single element types for clarity of correlation with analytic and experimental results. The functionality of the pre-processor was developed for continued use with AMROC-DYNA.

The post-processor routine functions robustly for multiple bodies and combinations of hexagonal “brick” elements and quadrilateral thin shell elements. VisIt readily generates coupled field displays of any combination of calculated variables from the simulation results.

## 2.4 Conclusions – Recommendations

The coupling of ARMOC to DYNA3D within VTF has been successfully verified and validated. All final results obtained are in good agreement with analytic and experimental results. The work flow from CUBIT to the AMROC-DYNA input files is efficient and effective. The post-processor routine has been fully integrated into the AMROC-DYNA solution routine and generates VTK formatted files without user intervention and at a

minimum computational cost. VisIt readily displays coupled field results for any combination of fluid density, pressure, velocity, and solid displacement, velocity, and stresses.

At present, the capabilities of AMROC-DYNA enable accurate simulations when solid structures are modeled with hexagonal eight-node “brick” elements and thin structures are modeled with quadrilateral thin shells.

AMROC-DYNA can simulate extrusion unplugging events where the simulant plug is modeled by hexagonal solid elements of a viscoplastic/elastic material and a slide surface defined at the interface between the plug and the pipeline.

## **2.5 Future Work**

The level-set generation algorithm needs to be extended by means of incorporating an outer-hull algorithm to enable the coupling of emerging solid surfaces along crack faces and separated fragments with the fluid. This enhancement would allow the simulation of arbitrarily complex three-dimensional solid structures modeled with hexagonal solid and cohesive elements. Once such an extension is developed and implemented, appropriate verification and validation should be carried out to ensure full functionality of AMROC-DYNA within VTF.

Once verified and validated, the extended AMROC-DYNA will be suitable for simulation of erosive unplugging events where the simulant plug is modeled by hexagonal solid and cohesive elements of a viscoplastic/elastic material with a slide surface defined at the interface between the plug and the pipeline.

### 3. RESEARCH DESCRIPTIONS

---

#### 3.1 AMROC

The VTF developed by Deiterding et al. is a generic software framework for shock-driven FSI simulation that imposes embedded moving wall boundary conditions on a Cartesian fluid solver with a ghost fluid approach. DYNA3D is a nonlinear, explicit finite element code for analyzing the transient dynamic response of three-dimensional solids and structures. The fluid solver, AMROC (Adaptive Mesh Refinement in Object Oriented C++), and the solid solver, DYNA3D, exchange data only at the interface between disjointed computational domains after consecutive time steps.

For the test cases selected, where strong shocks dominate the flow regime, the following equations were compiled in AMROC's solver framework by Dr. Dieterding.

Euler equations

$$\frac{\partial \rho}{\partial t} + \frac{\partial}{\partial x_k}(\rho u_k) = 0$$

$$\frac{\partial}{\partial t}(\rho u_i) + \frac{\partial}{\partial x_k}(\rho u_i u_k + \delta_{ik} p) = 0$$

$$\frac{\partial E}{\partial t} + \frac{\partial}{\partial x_k}(u_k(E + p)) = 0$$

Stiffened gas equation of state

$$p = (\gamma - 1)(E - \frac{1}{2}u_k u_k) - \gamma p_\infty$$

Finite volume scheme

$$\mathbf{Q}_{jk}^{l+1} = \mathbf{Q}_{jk}^l - \frac{\Delta t}{\Delta x_1} (\mathcal{A}^- \Delta_{j+\frac{1}{2},k} + \mathcal{A}^+ \Delta_{j-\frac{1}{2},k}) - \frac{\Delta t}{\Delta x_2} (\mathcal{B}^- \Delta_{j,k+\frac{1}{2}} + \mathcal{B}^+ \Delta_{j,k-\frac{1}{2}})$$

In order to provide detailed solutions in regions of interest and accurate boundary pressures on the moving solid boundaries, fine local temporal and special grid resolutions must be generated. This is accomplished efficiently through the block-structured adaptive mesh refinement method (SAMR) by M. Berger and P. Colella (1988). AMROC (Adaptive Mesh Refinement in Object-oriented C++) provides SAMR to the VTF in a generic form within its framework (Deiterding, 2002) that can be used in parallel systems that utilize the MPI library. An example of the spatial grid refinement and hierarchy is shown in Figure 6. Subgrids are computationally decoupled through the use of ghost cells. Figure 7 shows an example of the regridding of finer levels as time progresses.

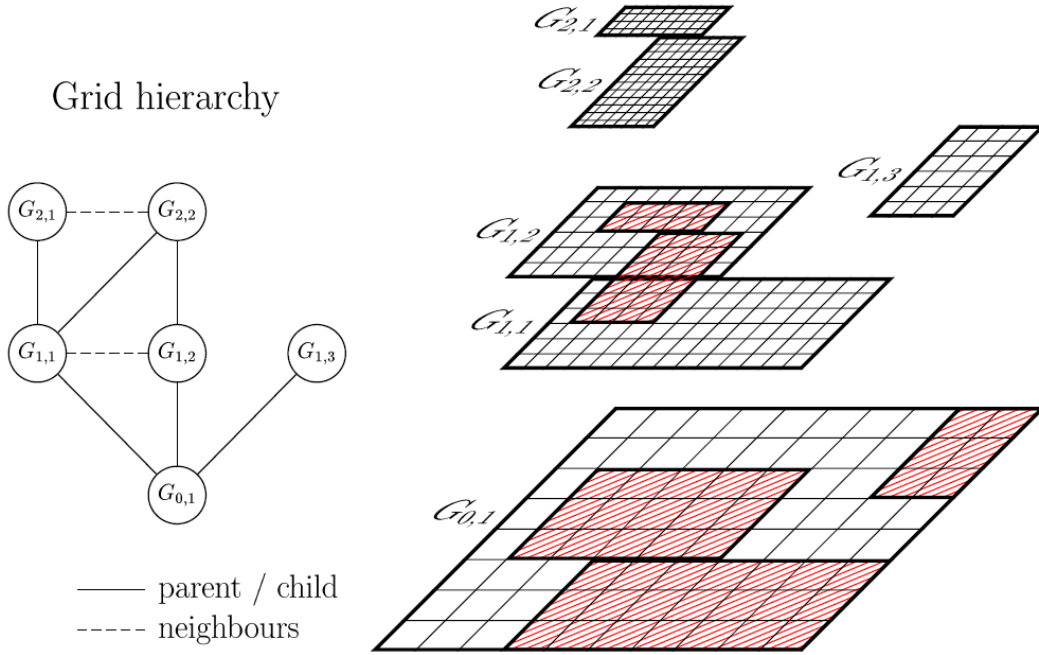


Figure 6. AMROC grid refinement hierarchy.

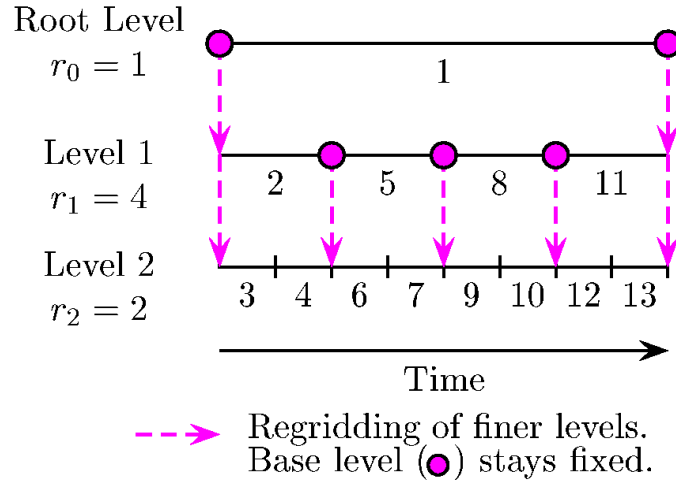


Figure 7. AMROC regridding strategy.

### 3.2 DYNA3D

DYNA3D is based on a finite element discretization of the three spatial dimensions and a finite difference discretization of time. DYNA3D uses a lumped mass formulation for efficiency. This produces a diagonal mass matrix  $\mathbf{M}$ , which renders the solution of the momentum equation:

$$\mathbf{M} \mathbf{a}_{n+1} = \mathbf{f}^{ext} - \mathbf{f}^{int}$$

trivial at each step in that no simultaneous system of equations must be solved.

The basic continuum finite element in DYNA3D is the eight-node “brick” solid element. This element is valid for large displacements and large strains. The element may be degenerated to a wedge or tetrahedral element, but at the expense of accuracy. Thus, these degenerated elements should be avoided whenever possible. (Lawrence Livermore National Laboratory, 2005). The brick element type was found to be the most accurate solid element type for the high deformation and strain rates present in both test cases. The release of DYNA3D utilized also supports five quadrilateral 4-node shell elements which can be degenerated to a triangular three-node element, but at the expense of accuracy. The triangular elements formed from collapsed quadrilaterals were found to lock due to excessive transverse shear, yielding non-physical results. The quadrilateral four-node shell and eight-node “brick” elements produced results which are in good agreement with the Euler-Bernoulli beam equation and each other. The same element types produced results in good agreement with the experimental results for the plate deformation from water hammer experimental results.

DYNA3D supports numerous material models suitable for a variety of materials and loading regimes. The kinematic/isotropic plasticity material model was well suited for the steel and copper structures of the verification and validation test cases because the shocks were severe enough to cause elastic and plastic deformation but not fracture.

The parameters of the kinematic/isotropic elastic-plastic model include the following:

Young’s modulus,  $E$

Poisson’s ratio,  $\nu$

Yield stress,  $\sigma_0$

Tangent modulus,  $E_T$

Hardening parameter,  $\beta$

The yield condition of the model can be written as

$$\phi = \bar{\sigma} - \sigma_y(\bar{\epsilon}^p)$$

where  $\bar{\sigma}$  is the effective stress and  $\sigma_y$  is the current yield stress, which may be a function of the effective plastic strain if strain hardening is included. For isotropic hardening, the effective stress  $\bar{\sigma}$  is given by:

$$\bar{\sigma} = \sqrt{\frac{3}{2} s_{ij} s_{ij}},$$

where  $s_{ij}$  is the deviatoric stress tensor. For kinematic hardening:

$$\bar{\sigma} = \sqrt{\frac{3}{2} \eta_{ij} \eta_{ij}}$$

where the translated stress  $\eta_{ij}$  is defined as:

$$\eta_{ij} = s_{ij} - \alpha_{ij},$$

and  $\alpha_{ij}$  is the (deviatoric) back stress tensor.

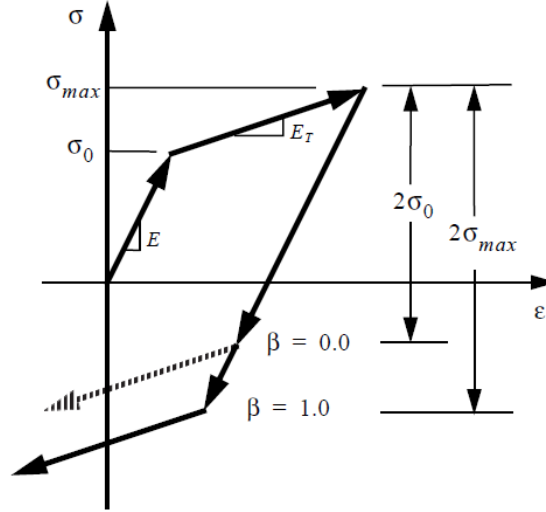


Figure 8. Uni-axial stress-strain relationship.

The linear isotropic hardening law has the form:

$$\sigma_y = \sigma_0 + \beta E_p \bar{\epsilon}^p,$$

where  $\sigma_y$  is the current yield stress,  $\sigma_0$  is the initial yield stress, and  $E_p$  is the plastic modulus.

The uni-axial stress strain curve in Figure 8. Uni-axial stress-strain shows the elastic-plastic material behavior for kinematic hardening ( $\beta = 0.0$ ) and for isotropic hardening ( $\beta = 1.0$ ).

The effective plastic strain is given by:

$$\bar{\epsilon}^p = \int_0^t d\bar{\epsilon}^p,$$

where the incremental effective plastic strain  $d\bar{\epsilon}^p$  is found from the incremental plastic strain tensor  $d\epsilon_{ij}^p$  as:

$$d\bar{\epsilon}^p = \frac{2}{3} d\epsilon_{ij}^p d\epsilon_{ij}^p \frac{1}{2}$$

The plastic modulus is found from Young's modulus  $E$  and the tangent modulus  $E_T$  using:

$$E_p = \frac{E E_T}{E - E_T}$$

The plastic hardening modulus  $E_p$  is the slope of the inelastic portion of the effective stress  $\bar{\sigma}$  vs. effective plastic strain  $\bar{\epsilon}^p$  curve. Similarly, the tangent modulus  $E_T$  is the slope of the inelastic part of a uniaxial stress  $\bar{\sigma}$  vs. strain  $\bar{\epsilon}^p$  curve (or equivalently, the effective stress vs. effective strain curve).

Kinematic and isotropic hardening elastoplastic models yield identical behavior under monotonic loading. Under reversed loading from a maximum stress  $\sigma_{\max}$ , kinematic hardening predicts reverse yielding when the stress has unloaded by an amount  $2\sigma_0$ , and isotropic hardening predicts that reverse yielding occurs when the stress reaches  $-\sigma_{\max}$ . Thus, under cyclic loading conditions where many stress reversals may occur, kinematic hardening predicts an hysteretic energy dissipation, while isotropic hardening predicts no energy dissipation after the first cycle. The isotropic model is slightly faster in computation speed, however (Lawrence Livermore National Laboratory, 2009).

### 3.3 Fluid Structure Coupling

The fluid solver, AMROC (Adaptive Mesh Refinement in Object Oriented C++), and the solid solver, DYNA3D, exchange data only at the interface between disjointed computational domains after consecutive time steps. Figure 9 shows the data flow within AMROC-DYNA from the initialization of the solution process to the iterative scheme of the coupled solver. The initialization parameters are listed within the hexagons at the top of the figure.

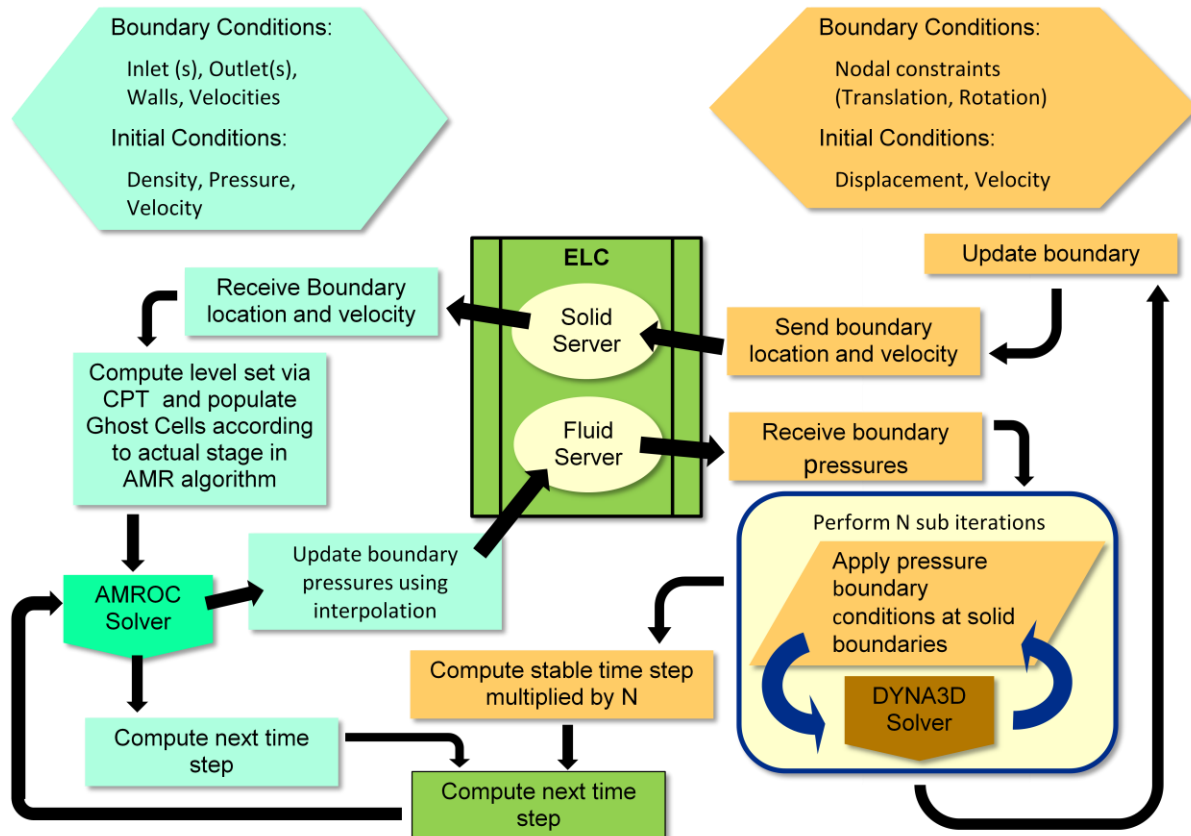


Figure 9. AMROC-DYNA data flow.

The coupling between AMROC and DYNA3D is established by enforcing the following compatibility conditions between inviscid fluid and solid at a slip interface:

- Continuity of normal velocity:  $u_n^S = u_n^F$
- Continuity of normal stresses:  $\sigma_{nn}^S = -p^F$
- No shear stresses:  $\sigma_{n\tau}^S = \sigma_{n\omega}^S = 0$

A time-splitting approach is applied for the coupling of the:

- *Fluid:*
  - Treats evolving solid surface with moving wall boundary conditions in fluid
  - Uses solid surface mesh to calculate fluid level set
  - Uses nearest velocity values  $\mathbf{u}^S$  on surface facets to impose  $u_n^F$  in fluid
- *Solid:*
  - Use interpolated hydro-pressure  $p^F$  to prescribe  $\sigma_{nn}^S$  on boundary facets

This coupling approach, which utilizes disjointed computational domains, allows Ad-hoc separation in dedicated fluid and solid processors. Figure 10 shows the associations of fluid cell centers (dots) and solid cell centers (x) across the solid surface. The associations direct the mapping of solid surface nodes to fluid cells as indicated by the blue arrows.

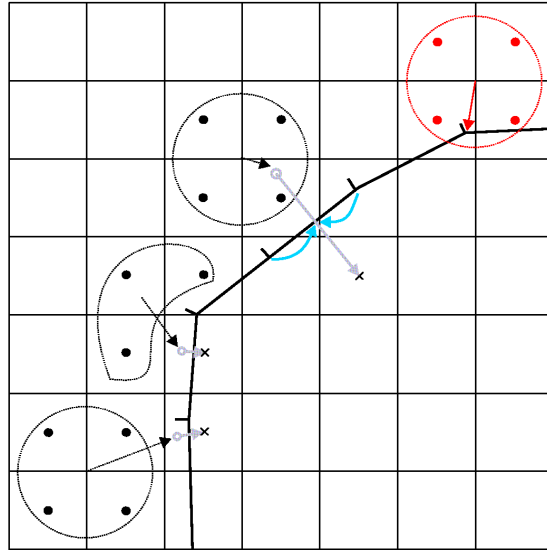


**Figure 10. Coupling surface.**

As the test cases were formulated into input files for DYNA3D and AMROC through manual text input, careful notes were made of the geometry processing which was necessary to translate the data of meshed body into the needed formats. CUBIT, developed by Sandia National Laboratory, was identified as a strong candidate for a mesh generator by Dr. Ralf Deiterding. CUBIT's capabilities to generate and mesh geometry were examined along with its export formats (Sandia National laboratory, 2008). The Abaqus file format was selected for its inclusion of node selection sets which would allow nodes to be identified for boundary conditions to be applied in DYNA and AMROC.

- Geometry pre-processor routine:
  - *Reads output from Cubit 11.0 Mesh Generator and dynamically creates a DYNA3D input file*
  - *Supports hexagonal, tetrahedral, thick shell , and thin shell elements*
  - *Translates node selection sets to apply boundary conditions, pressure loads on included faces, and generates cohesive elements for fracture simulation*

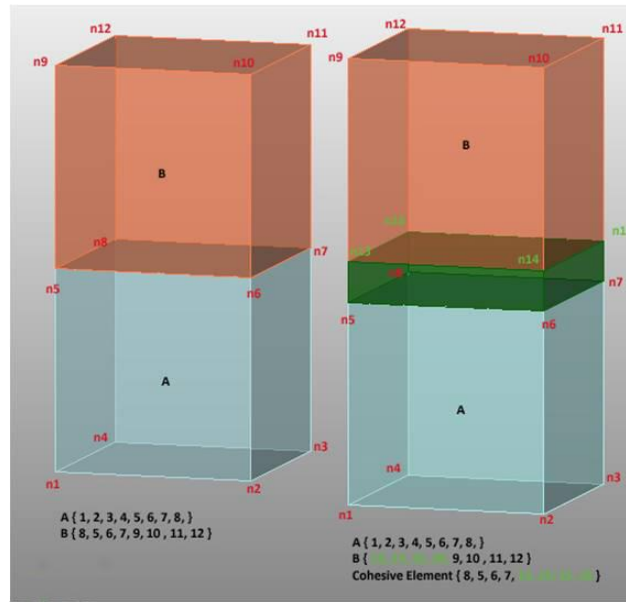
#### **Node selection sets**

- 1 – 9999 : identify volumes where cohesive elements are to be generated to simulate possible fracture(s)
- 10000 – 19999 : identify nodes to which translation and rotation nodal constraints will be applied
- 20001 – 29999 : identify nodes on surfaces where pressure loads will be applied

#### **Cohesive elements**

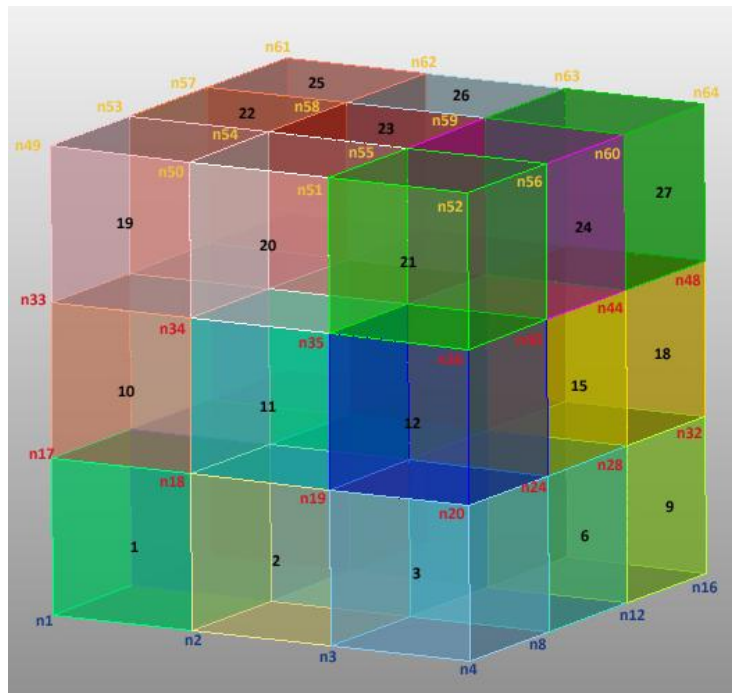
- used to simulate cohesion or inter-laminar forces between “parallel” hex elements
- employ traction-displacement relationships to generate nodal forces based upon the projected displacements of the hex element corners in opening (mode I) and in plane shear (mode II) directions

Figure 11 shows the generation of new initially coincident nodes between two arbitrary elements to create cohesive elements. The generation of new nodes prompts updates of the mapping of nodes to elements and faces in order to preserve nodal constraints and pressure loads. The thickness of cohesive element is a visual aide only.



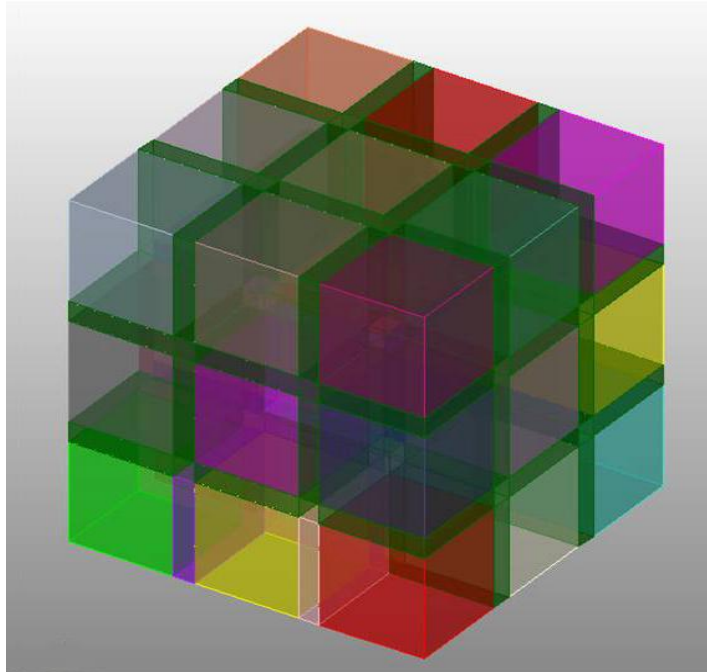
**Figure 11. Generation of a cohesive element.**

Figure 12 shows an exemplary volume discretized by hexagonal elements and designated with the following node selection sets: 1 = Cohesive element generation (all), 10700 = Nodal constraint: translation fixed in x,y,z (blue), 20001 = Pressure loaded faces (yellow)



**Figure 12. Node selection sets.**

Figure 13 shows the generated cohesive elements within the exemplary mesh of solid hexagonal elements to model possible fracture. The thickness of cohesive elements is a visual aide only.



**Figure 13. Generated cohesive elements.**

A literature search of FSI software validation and FSI experimental publications was undertaken in parallel with an examination of the DYNA3D manuals (Lawrence Livermore National Laboratory, 2005), examples, and publications cited (Sanjay Govindjee, 1995) by the developers. The publications of (A. Neuberger, 2009), (Boyd, 2000), (Deshpande, Heaver, & Fleck, 2006), (Michael J. Hargather, 2007), and (M.J. Hargather, 2009) were most helpful in familiarizing the DOE Fellow with the experimental techniques and approximations utilized to examine the response of shock-loaded structures. Notably, the approximations between explosive materials and the impulse imparted to the structure were found to be focused on the permanent deformation of the structure. The publications of (Ralf Deiterding, 2008), (Boris Stok, 2009), and (Z. Zong, 2001) were instructive in the analytic and finite element modeling techniques applicable to studying the FSI of shock-loaded structures. The publications of (Chelluru, 2007), (Sanjay Govindjee, 1995), (Tabiei, 2009), (W.G. Jiang, 2005), and (Zhang, 1999) were instructive in the finite element techniques employed to model fracture and crack propagation.

Test cases were selected from the experiments and simulations surveyed which had detailed material data and results for both the plastic and elastic response of a structure subjected to a strong shock in water or air.

### **3.4 Verification Test Case: Shock-induced Panel Motion**

The computational domain of the verification test case can be seen in Figure 14. The region of high density, high velocity, and high pressure fluid is at the left of the domain approaching the forward facing step ahead of the steel panel which is surrounded by quiescent air at atmospheric pressure. The panel is located 1.5 cm behind the step. Reflective boundaries conditions are applied everywhere except at the inflow on the left of the domain.

- Elastic motion of a thin steel plate (thickness  $h=1\text{mm}$ , length  $50\text{mm}$ )
- Steel plate modeled with finite difference solver using the beam equation

$$\rho h \frac{\partial^2 w}{\partial t^2} + EI \frac{\partial^4 w}{\partial x^4} = p(x, t)$$

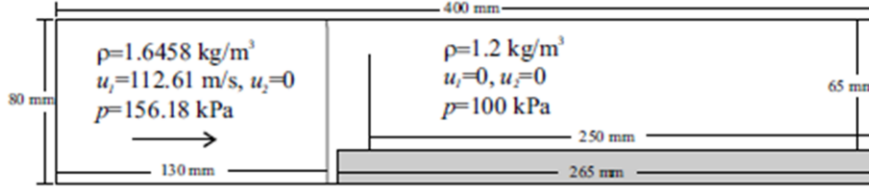


**Figure 14. Verification Test Case computational domain.**

For the initial verification of the implementation of DYNA3D, low to moderate loading was applied to the steel panel structure to yield purely elastic responses. Accordingly, elastic materials were applied within the simulation. For higher loadings, viscoplastic/elastic and failure material types were evaluated for their accuracy and computational cost. AMROC was run with a SAMR base mesh  $320 \times 64 (x2)$ , utilizing 2 additional levels of adaptive refinement with factors 2, 2.

As the interaction of stronger shock with structures were examined for the validation test case and experimental results indicated fracture was likely, DYNA3D's cohesive elements were tested and implemented within the pre-processor through a cohesive node selection set. To produce stable solutions for these simulations of higher deformation rates, several DYNA3D solver parameters had to be examined and fine tuned. Most prominent of these being the set of hour-glass stabilization parameters, the time-step scale factor, the slide surface coefficients, and the cohesive element properties.

### 3.5 Validation Test Case: Plate Deformation from Water Hammer

This test case is a 3-D simulation of plastic deformation of thin copper plate attached to the end of a pipe due to water hammer. Strong over-pressure wave in water is induced by rapid piston motion at end of tube as described in experiments from 'An underwater shock simulator', V.S. Deshpande et al. A two-component model based on a "stiffened" gas equation of state was implemented to enforce the attenuation of the pressure wave as observed in the experiments due to viscous effects (see Figure 16). Computations were performed with the following parameters  $\gamma^{Air}=1.4$ ,  $p_1^{Air}=0$ ,  $\gamma^{Water}=7.415$ ,  $p_1^{Water}=2962$  bar. Cavitation modeling was included with a pressure cut-off at  $p=0$  MPa, and surface tension was neglected. Realistic pressure loading in simulations were created by solving equation of motion for the piston. Figure 15 shows the experimental setup utilized by Deshpande et al.

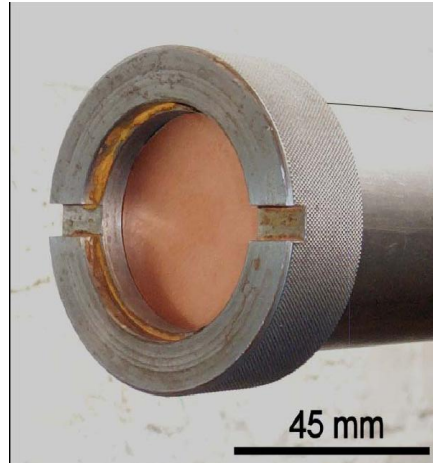


Figure 15. AMROC-DYNA validation experimental setup.

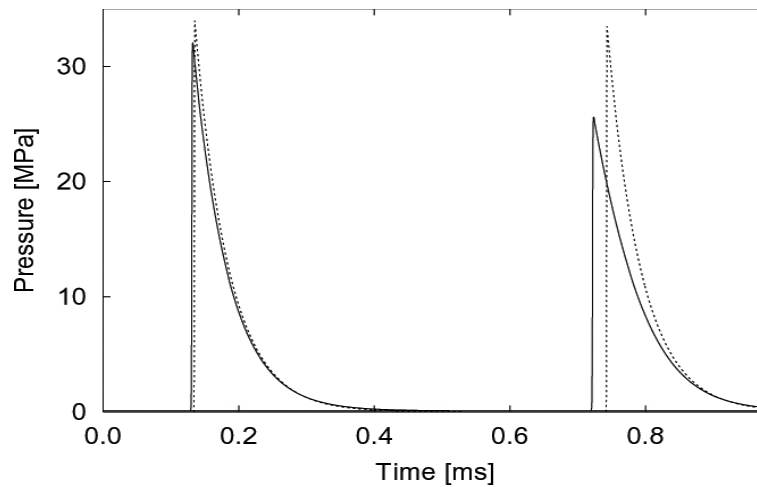


Figure 16. Comparison of the traveling wave approximation (dotted) with computed pressure traces (solid) at  $x_1 = 1.1$  m (left) and  $x_1 = 0.2$  m (right).

### 3.6 Fracture Demonstrations

The strongest over-pressure waves in water is induced by rapid piston motion at end of tube as described in experiments from ‘An underwater shock simulator’, V.S. Deshpande et al., 2006, causing the copper plate to fracture in distinct patterns. Cases such as these where the fluid structure interaction caused high rates of deformation in thin structures and ultimately fracture were simulated successfully for thin structures modeled with solid hexagonal elements, cohesive elements, and slide surfaces. The restriction to thin structures, that is, those structures which can be represented in the fluid domain by unsigned distance functions, is enforced because at present the algorithm implemented to generate the level sets from the solid surface does not capture new surfaces along crack faces. The results obtained are in agreement with the observed experimental results.

## 4. RESULTS AND ANALYSIS

### 4.1 Routines

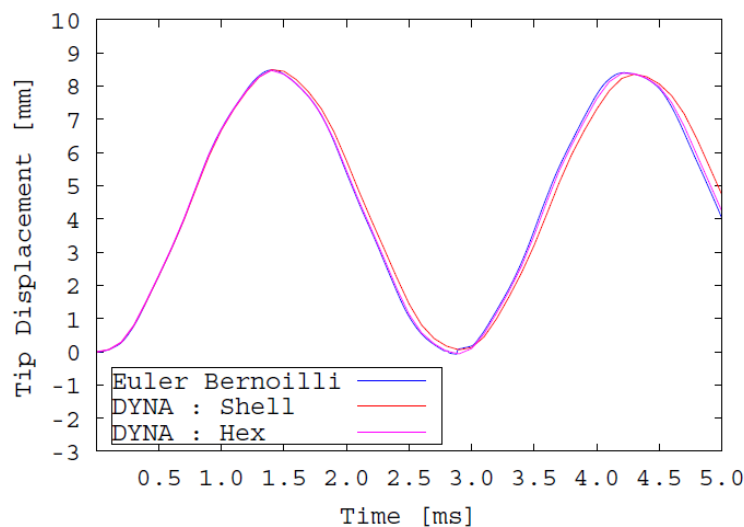
The geometry pre-processor routine functions robustly for multiple bodies and element types. The test cases employed for verification and validation were of single body, single element types for clarity of correlation with analytic and experimental results. The functionality of the pre-processor was developed for continued use with AMROC-DYNA.

The post-processor routine functions robustly for multiple bodies and combinations of hexagonal "brick" elements and quadrilateral thin shell elements. VisIt readily generates coupled field displays of any combination of calculated variables from the simulation results.

### 4.2 Verification Test Cases

- DYNA3D implementation verification: constant impulsive loading of  $\Delta p = 100 \text{ kPa}$ 
  - *Euler-Bernoulli Beam Equation*
  - *DYNA : Shell: DYNA3D explicit finite element solver employing thin-shell elements*
  - *DYNA : Hex: DYNA3D explicit finite element solver employing hexagonal elements*

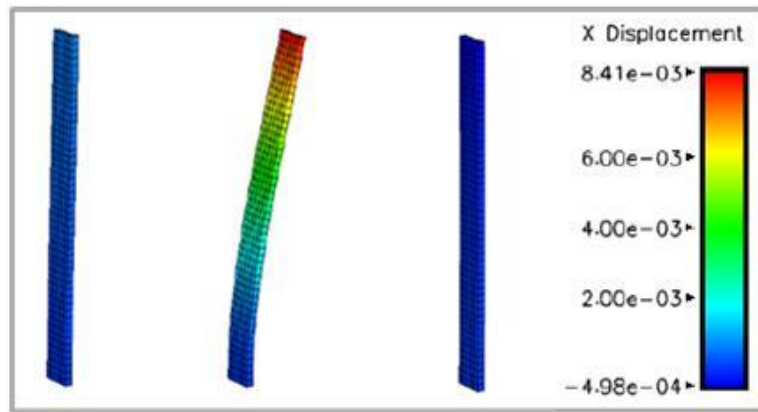
The quadrilateral four-node shell and eight-node "brick" elements produced results which are in good agreement with the Euler-Bernoulli beam equation and each other. Figure 17 shows the time history of the 5 x 50 x 0.1 cm steel panel's tip displacement loaded with 100 kPa on one side.



**Figure 17. DYNA3D verification.**

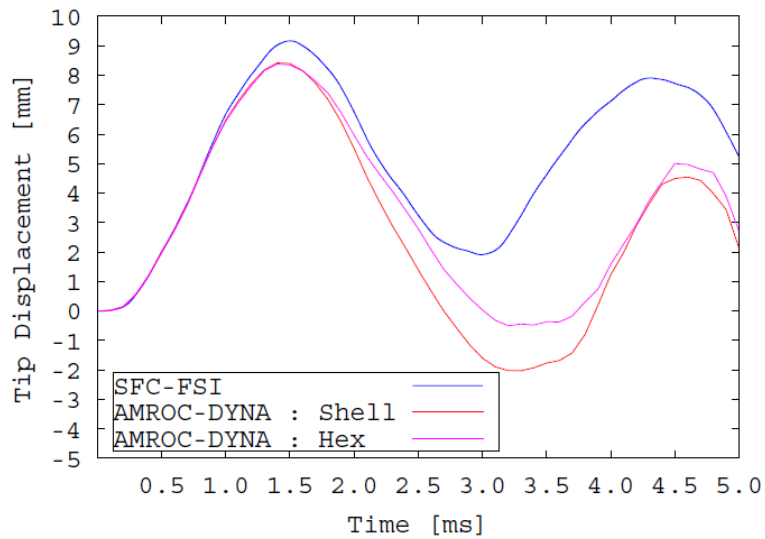
- FSI verification:
  - *SFC-FSI: large displacement thin-shell finite element solver by F.Cirak coupled to FV code*
  - *AMROC-DYNA : Shell: DYNA3D explicit finite element solver employing thin-shell elements coupled to AMROC*
  - *AMROC-DYNA : Hex: DYNA3D explicit finite element solver employing hexagonal elements coupled to AMROC*
- Intel 3.4GHz Xeon dual processors connected with Gigabit Ethernet
  - *SFC-FSI: 12.25h CPU on 3 fluid CPU + 1 solid CPU*
  - *AMROC-DYNA : Hex: 600h CPU 15 fluid CPU + 1 solid CPU*
  - *AMROC-DYNA : Shell: 450h CPU 15 fluid CPU + 1 solid CPU*

Figure 18 shows the hexagonal mesh of the 5 x 50 x 0.1 cm steel panel colored for x displacement at time 0.3, 1.4, and 3.2 ms.



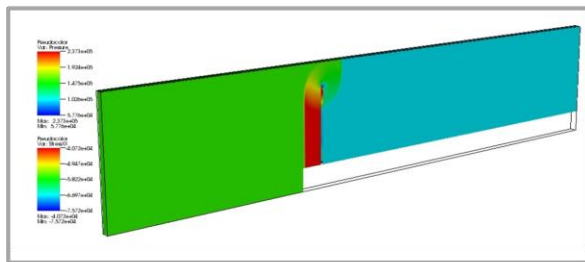
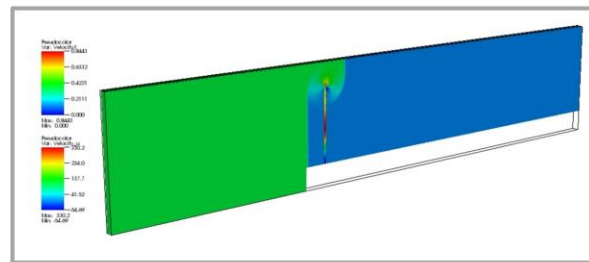
**Figure 18. AMROC-DYNA panel displacement.**

Figure 19 shows the time history of the 5 x 50 x 0.1 cm steel panel's tip displacement loaded with the dynamic pressures calculated by AMROC.

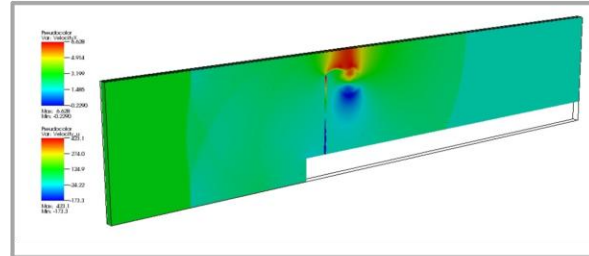
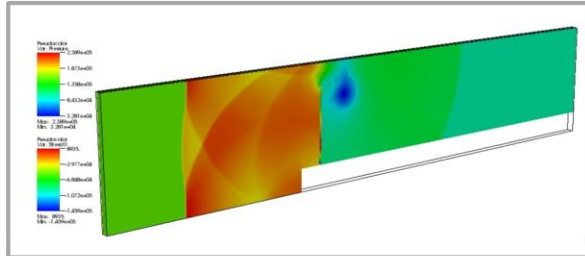


**Figure 19. AMROC-DYNA verification.**

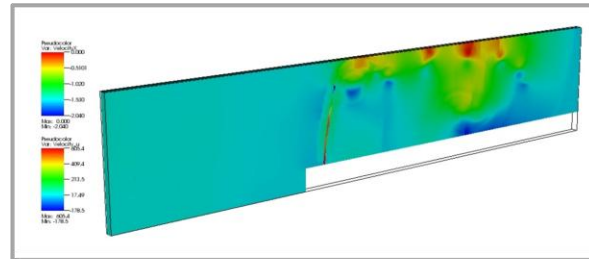
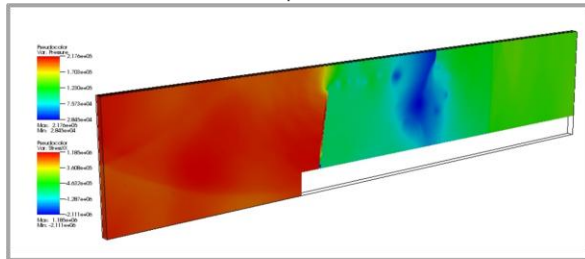
Figure 20 shows the time history of the shockwave interaction with the steel panel displaying the fluid pressure and panel stress in the left column and the fluid and panel velocity along the channel axis x.

**Fluid Pressure and Solid Stress XX****Fluid and Solid velocity  $u_x$** 

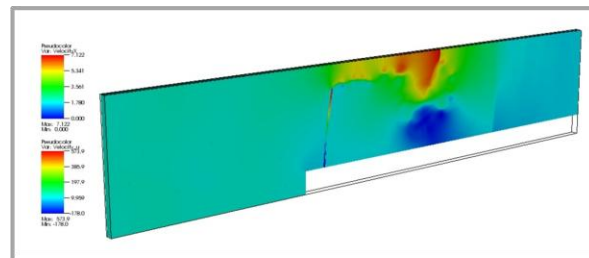
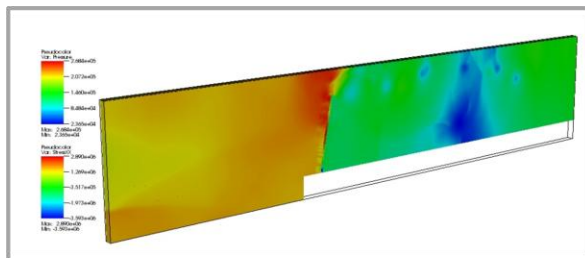
Time = 0.3 ms Shockwave impact on panel



Time = 0.6 ms Reflected pressure wave



Time = 1.4 ms maximum panel deflection



Time = 3.2 ms maximum panel rebound

**Figure 20. AMROC-DYNA verification panel motion coupled field results.**

### 4.3 Validation Test Cases

The quadrilateral four-node shell and eight-node “brick” elements produced results which are in good agreement with the experimental results from the plate deformation from water hammer experiments. The cavitation from 0.06 to 0.2 ms following the initial impact of the shock wave on the plate can be readily discerned in Figure 21, Figure 22, and Figure 23.

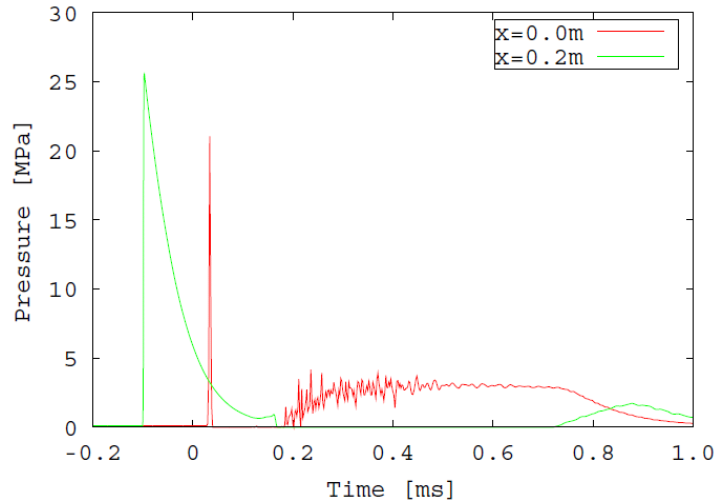


**Figure 21. Pressure traces along centerline.**

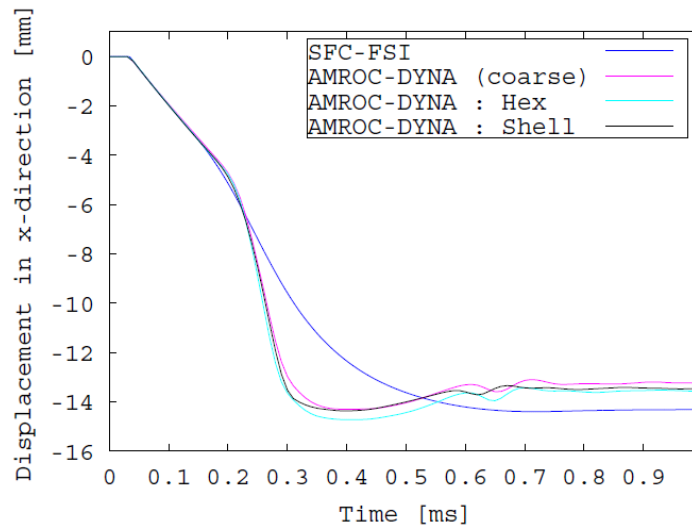


**Figure 22. Plate centerline x-displacement.**

- FSI validation:
  - *SFC-FSI: large displacement thin-shell finite element solver by F.Cirak coupled to FV code*
  - *AMROC-DYNA : Shell: DYNA3D explicit finite element solver employing thin-shell elements coupled to AMROC*

- *AMROC-DYNA : Hex: DYNA3D explicit finite element solver employing hexagonal elements coupled to AMROC*
- Intel 3.4GHz Xeon dual processors connected with Gigabit Ethernet
  - *SFC-FSI: 130h CPU on 8 nodes*
  - *AMROC-DYNA: Hex: 206h CPU 15 fluid CPU + 1 solid CPU*
  - *AMROC-DYNA: Shell: 97h CPU 15 fluid CPU + 1 solid CPU*

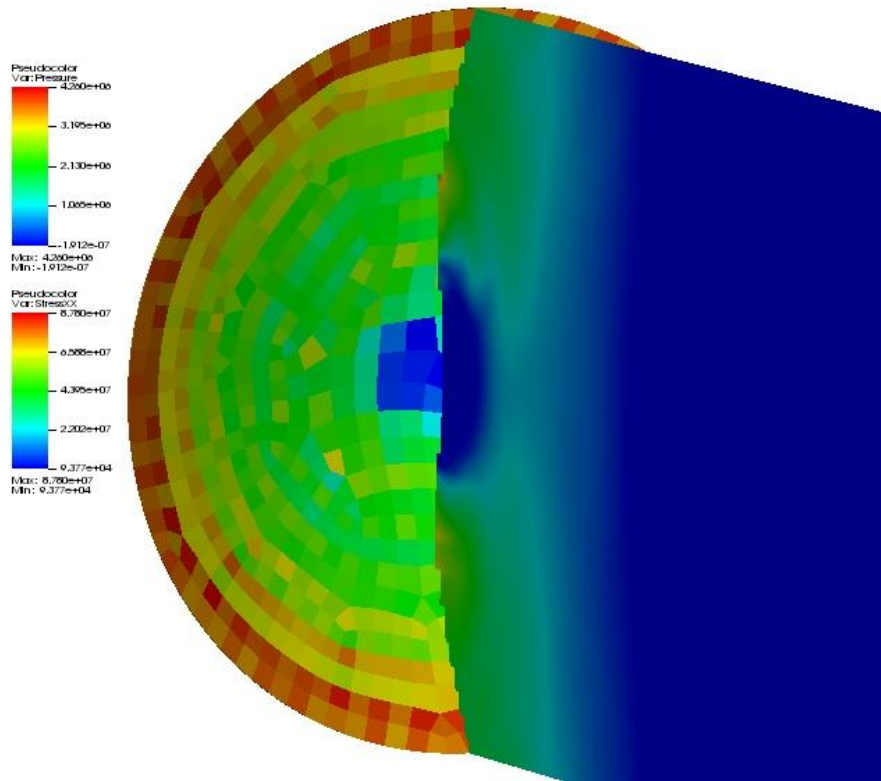
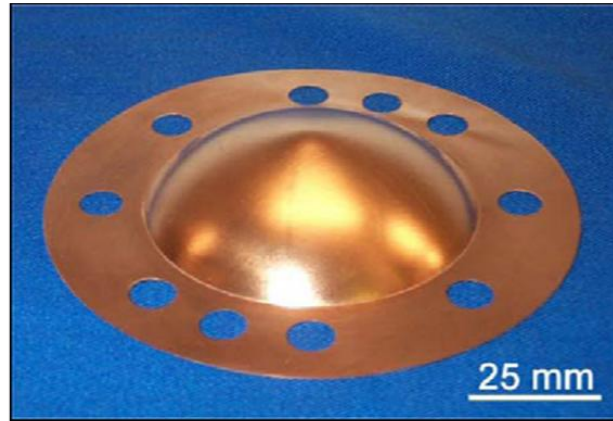
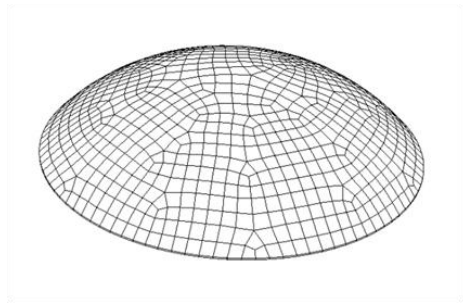


**Figure 23. Fluid pressure distribution revealing cavitation and stressXX distribution within the copper plate at  $t = 0.15$  ms.**

Figure 24 shows the comparison of the copper plate at the end of the experiment from Despande et. al.



**Comparison of plate at end of simulation and experiment show good agreement of shape and maximum deflection.**

**Figure 24. Comparison of AMROC-DYNA results with experiment results.**

#### **4.4 Fracture Demonstration**

3-D simulation of plastic deformation of thin copper plate attached to the end of a pipe due to strong water hammer were modeled with cohesive elements and sliding contact between solid elements. Preliminary results show agreement with experimental results as can be seen in Figure 25.

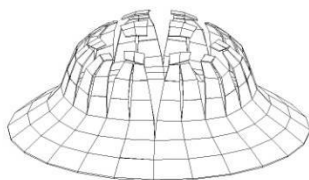
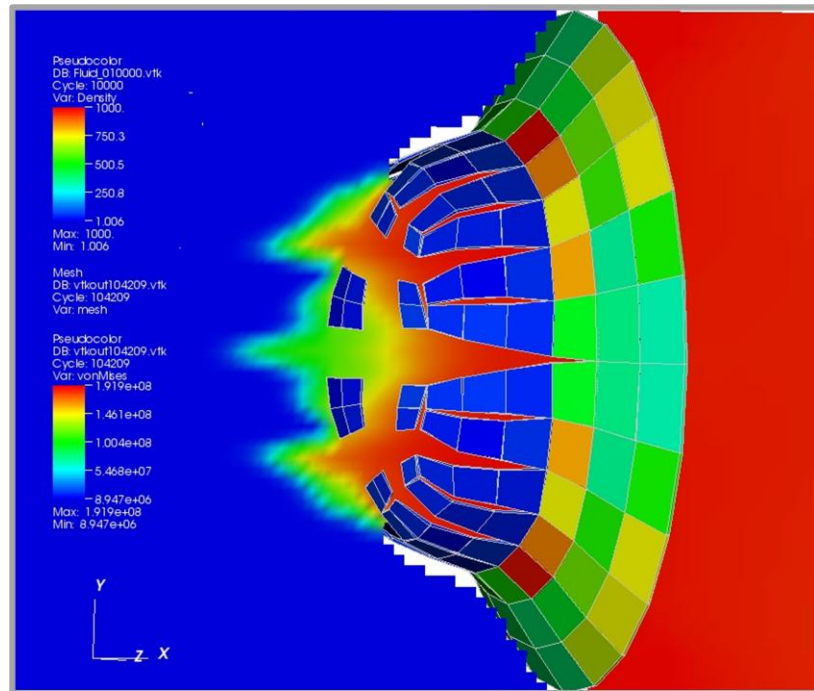


**Figure 25. Comparison of AMROC-DYNA fracture demonstration with experimental results.**

The flow of water and vapor through the fractured plate can be seen in Figure 26 where the denser water is red and the ambient air is blue.



Time = 1.0 ms

**Figure 26. Fluid density and plate von Mises stress.**

The dynamics of the fluid-structure interaction can be observed in the pictorial series in Figure 27.

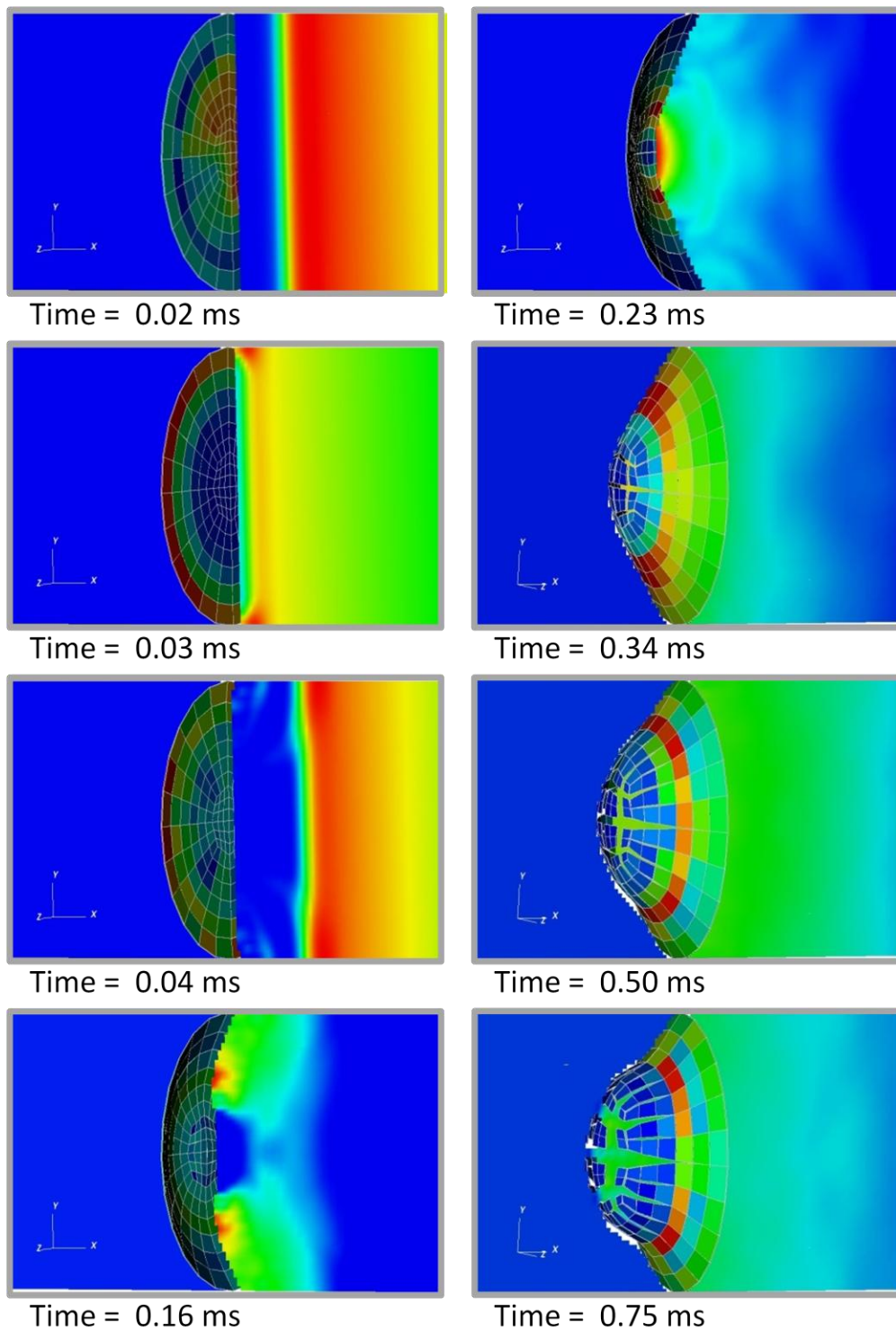


Figure 27. Fluid pressure and plate von Mises stress from behind the plate in left column and from in front of the plate in the right column.

## 5. CONCLUSION

---

The coupling of AMROC to DYNA3D within VTF has been successfully verified and validated. All final results obtained are in good agreement with analytic and experimental results. The work flow from CUBIT to the AMROC-DYNA input files is efficient and effective. The post-processor routine has been fully integrated into the AMROC-DYNA solution routine and generates VTK formatted files without user intervention and at a minimum computational cost. VisIt readily displays coupled field results for any combination of fluid density, pressure, velocity, and solid displacement, velocity, and stresses.

At present, the capabilities of AMROC-DYNA enable accurate simulations when solid structures are modeled with hexagonal eight-node “brick” elements and thin structures are modeled with quadrilateral thin shells.

AMROC-DYNA can simulate extrusion unplugging events where the simulant plug is modeled by hexagonal solid elements of a viscoplastic/elastic material and a slide surface defined at the interface between the plug and the pipeline.

### Future Work

The level-set generation algorithm needs to be extended by means of incorporating an outer-hull algorithm to enable the coupling of emerging solid surfaces along crack faces and separated fragments with the fluid. This enhancement would allow the simulation of arbitrarily complex three dimensional solid structures modeled with hexagonal solid and cohesive elements. Once such an extension is developed and implemented, appropriate verification and validation should be carried out to ensure full functionality of AMROC-DYNA within VTF.

Once verified and validated, the extended AMROC-DYNA will be suitable for simulation of erosive unplugging events where the simulant plug is modeled by hexagonal solid and cohesive elements of a viscoplastic/elastic material with a slide surface defined at the interface between the plug and the pipeline.

## 6. REFERENCES

---

- A. Neuberger, A. P. (2009). Springback of circular clamped armor steel plates subjected to spherical air-blast loading. *International Journal of Impact Engineering* , 53 - 60.
- Boris Stok, M. H. (2009). Analytical solutions in elasto-plastic bending of beams with rectangular cross section. *Applied Mathematical Modelling* , 1749-1760.
- Boyd, S. D. (2000). *Acceleration of a Plate Subject to Explosive Blast Loading - Trial Results*. Melbourne, Victoria, Australia: DSTO Aeronautical and Maritime Research Laboratory.
- Caltech ASC Center for Simulation of Dynamic Response of Materials. (n.d.). *The Virtual Test Facility*. Retrieved May 2009, from The Virtual Test Facility:  
<http://www.cacr.caltech.edu/asc/wiki/bin/view/>
- Chelluru, S. K. (2007). *Ffinite Element Simulations of Ballistic Impact on Metal and Composite Plates*. Wichita, Kansas: Wichita State University.
- Deshpande, V. S., Heaver, A., & Fleck, N. A. (2006). An underwater shock simulator. *Royal Society of London Proceedings Series A* , 1021–1041.
- John M. Brett, g. Y. (2008). A study of explosive effects in close proximity to a submerged cylinder. *International Journal of Impact Engineering* , 206-225.
- Lawrence Livermore National Laboratory. (2009, July). Retrieved 2009, from VisIt visualization tool: <https://wci.llnl.gov/codes/visit/home.html>
- Lawrence Livermore National Laboratory. (2005). *DYNA3D: A Nonlinear, Explicit, Three-Dimensional Finite Element Code for Solid and Structural Mechanics*. Livermore, CA: LLNL Methods Development Group Mechanical Engineering.
- Lawrence Livermore National Laboratory. (2009, May). *LLNL Engineering Methods Development Group Codes DYNA3D*. Retrieved from Engineering at LLNL: [https://www-eng.llnl.gov/mdg/mdg\\_codes\\_dyna3d.html](https://www-eng.llnl.gov/mdg/mdg_codes_dyna3d.html)
- M.J. Hargather, G. S. (2009). Laboratory-scale techniques for the measurement of a material response to an explosive blast. *International Journal of Impact Engineering* , 940-947.
- Michael J. Hargather, G. S. (2007). Optical measurement and scaling of blasts from gram-range. *Shock Waves* , 215-223.
- Office of River Protection. *09-006C-110*.
- Ralf Deiterding, F. C. (2008). Efficient Fluid-Structure Interaction Simulation of Viscoplastic and Fracturing Thin-Shells Subjected to Underwater Shock Loading. *Fluid-Structure Interaction. Theory, Numerics and Applications* , 65 - 80.
- Sandia National laboratoy. (2008). *CUBIT 11.1 User Documentation*. Retrieved June 2009, from CUBIT: <http://cubit.sandia.gov/help-version11.1/cubithelp.htm>
- Sanjay Govindjee, G. J. (1995). Anisotropic Modelling and Numerical Simulation of Brittle Damage in Concrete. *International Journal for Numerical Methods in Engineering* , 3611-3633.
- Tabiei, S. A. (2009). Automated dynamic fracture procedure for modelling mixed-mode crack propagation using time integration brick finite elements. *Fatigue & fracture of Engineering Materials & Structures* , 357-377.
- Visualization Tool Kit. (2009). Retrieved July 2009, from VTK- The Visualization Toolkit: <http://www.vtk.org/>

- W.G. Jiang, S. H. (2005). Modelling of damage in composite materials using interface elements. *5th European LS-DYNA Users Conference*. Birmingham, UK: DYNAlook.
- Z. Zong, K. Y. (2001). Viscoplastic response of a circular plate to an underwater explosion shock. *ACTA Mechanica* , 93-104.
- Zhang, L. (1999). On the separation criteria in the simulation of orthogonal metal cutting using the finite element method. *Materials Processing Technology* , 273-278.